Highly Accurate Technique for CO-OFDM Channel Estimation Technique Using Extreme Learning Machine (ELM)

NISHA MARY JOSEPH, PUTTAMADAPPA C.
Department of Electronics and Communication Engineering, Dayananda Sagar University,
Kudlu gate, Hosur, Bangalore,
INDIA

Abstract: - In wireless systems, channel estimation is considered a problematic technology, due to the fact of the difference in time between wireless channels and the noise effect. Orthogonal frequency-division multiplexing (OFDM) is a promising candidate for future optical communications and has received wide concern. The article proposed a Coherent Optical (CO) orthogonal frequency division multiplexing (OFDM) scheme, which gives a scalable and flexible solution for increasing the transmission rate, being extremely robust to chromatic dispersion as well as polarization mode dispersion. Nevertheless, both coherent detection and OFDM are prone to phase noise due to the phase mismatch between the laser oscillators at the transmitter and receiver sides and the relatively long OFDM symbol duration compared to that of single carrier communications. An Extreme Learning Machine (ELM) with Pilot Assisted Equalization (PEM) is proposed for compensation of impairments caused by fibre nonlinearity in coherent optical communication systems. Channel estimation using ELM and the value of distortion is sent to the OSTBC receiving end based on the distortion information the data is decoded and pilot data is removed. FFT is applied to the data and QPSK demodulation is done in the data to get its original form. In addition, the article utilized a free-space optical communication system of multi-input multi-output orthogonal frequency division multiplexing (MIMO-OFDM) with a modified receiver structure. Simulation reveals that the proposed model exhibits significant BER (0.0112) performance and provides better spectral efficiency as compared with conventional systems and less computational complexity. This suggested that the proposed method shows better performance by using the CO-OFDM-FSO-MIMO-ELM-based channel estimation technique for high-speed data communication networks in real-time scenarios respectively.

Keywords: - Optical Networks, Coherent Optical Orthogonal Frequency Division Multiplexing, Channel Estimation, Extreme Learning Machine, Bit Error Rate and Channel Equalization.

Received: April 4, 2022. Revised: January 6, 2023. Accepted: February 12, 2023. Published: March 9, 2023.

1 Introduction

Over the past few decades, global network traffic has grown explosively due to the demands for higher bandwidth and faster connections of various multimedia and data services (e.g. big data, cloud computing, streaming video, Internet of Things, machine-to-machine communication, and remote surgery), [1]. Conventional cable-based transmission approaches cannot meet the enormous data transmission requirements. With the advantages of low loss, large bandwidth, and anti-electromagnetic interference, optical fibres have replaced cables and have been widely used as the transmission medium in fiber-to-the-home (FTTH) networks, metropolitan area networks (MANs), backbone networks, and transoceanic communications, [2]. Due to the wide application of fibre-optic networks, optical fibres exist anywhere in modern society, and fibre can be exploited for more functions than data transmission. In addition to acting as the transmission medium in fibre-optic networks, optical fibre can also act as the sensing medium in optical fibre sensors, [3]. The fibre channel model plays an essential role in the simulation and design of optical fibre communication systems. However, it is difficult for conventional model-driven modelling to balance accuracy and efficiency, especially in optical orthogonal frequency division multiplexing (OFDM) systems with complex and long-haul transmission, [4]. Orthogonal frequency-division multiplexing (OFDM) is a widely used modulation/multiplexing technology in wireless and data communications. With recent advances in high-speed CMOS technologies and optical modulation and detection technologies, optical OFDM at 40-Gb/s or even 100-Gb/s information rate becomes feasible. Together with digital coherent detection,

coherent optical OFDM (CO-OFDM) brings similar benefits such as high spectral efficiency and high receiver sensitivity as coherent single-carrier transmission, [5]. A key feature of CO-OFDM is its capability to insert training symbols (TS's) at the transmitter to facilitate channel estimation, which provides crucial information about the transmission channel and enables efficient digital compensation of optical transmission impairments such as chromatic dispersion (CD) and polarization-mode dispersion (PMD). High peak-to-average power ratio (PAPR) remains the main challenge of coherent optical orthogonal frequency division multiplexing (CO-OFDM) systems. Due to the strong properties of selective frequency fading channels, the research attention has been admired by the OFDM transmission, [6].

Orthogonal frequency division multiplexing (OFDM) technology and multi-input multi-output (MIMO) technology are widely used in wireless communication systems, improving spectral efficiency, data transmission quality, and system capacity, [7]. In MIMO-OFDM wireless communication systems, the channel state information (CSI) obtained by channel estimation techniques is critical, as it has a significant impact on the accurate implementation of coherent detection and decoding and directly guides the configuration of analogue and digital beam formers, [8]. Currently, complex and extensive application scenarios and exponentially growing data volumes are placing increasingly high demands on the data transmission rate and latency of the systems (e.g., 5 G requires 10-Gbits/s ~ 20-Gbits/s peak rate and sub-1 ms round-trip latency), [9]. Especially in channel estimation, an increasing number of channel coefficients and long pilot sequences need to be trained, and increasingly stringent latency constraints are imposed. These pose growing challenges to existing channel estimation based on electronic processors in terms of computing power proportional to parallelism, data storage, and data transmission, [10]. Specifically, channel estimation entails large-scale complex matrix computations, which in turn, requires a large number of transistors working together and additional scheduling procedures to coordinate the movement of data involving weights, resulting in an overall latency on the order of milliseconds. Besides, in other electrical signal processing associated with channel estimation (e.g., serial-to-parallel conversion and fast Fourier transform), there is additional latency of microseconds in signal access, processing, storage, and transmission, [11]. Thus, key performances of channel estimation still have room for improvement in terms of computational speed, latency, and parallelism and our research aims to reduce the latency of the entire channel estimation process and improve the computational speed and parallelism of channel estimation.

Channel estimation schemes based on the interference approximation method (IAM) have been proven to be effective in suppressing the IMI with low complexity, [12]. For the IAMs, increasing the power of the pseudo pilot could decrease the effects of amplified spontaneous emission (ASE) noise and other frequency domain residual errors on the channel estimation accuracy. In most of the previously reported IAM works, pilot blocks were designed according to the structure of the centre pilot block loaded, while the two side pilots nulled for simplicity. However, the power of the pseudo pilot under this method did not reach the maximum, resulting in non-optimal channel estimation accuracy. Recently, Xi Fang suggested the channel estimation model based on the combined phase offset (CMPO). For the CMPO method, the first and the third pilot blocks are also loaded with pilots. With this consideration, a pilot structure called E-IAM-C was proposed for OFDM/OQAM, improving the pseudo pilot power compared with the IAMs and PHO, [13]. However, for the E-IAM-C method, matrix inversion is required due to the restriction for time domain channel estimation approaches, leading to high computational complexity (Ling Yang, 2021). CO-OFDM has many advantages, including scalability to the ever-increasing data rate and transponder adaptability, high receiver sensitivity and spectral efficiency, and robustness against dispersion. However, the impact of the optical channel is a major limiting factor in CO-OFDM systems when the speed rate is up to 100 Gbit/s or higher. Therefore, it requires to use of effective channel estimation methods to track the channel changes. Accurate channel estimation is the key factor to improve the receiver quality, and it is also the main requirement to improve the transmission performance of CO-OFDM systems, [14]. Nevertheless, channel estimation has attracted limited attention in the field of CO-OFDM systems in recent years. Many channel estimation methods were reported in the CO-OFDM system, such as least square (LS), maximum likelihood (ML), linear minimum mean square error (LMMSE) algorithms, and deep neural network, [15]. Recently, a neural network, [5] was used as a nonlinear model to approximate the relationship between the channel impulse response and its corresponding subcarrier index. Most semi-blind estimation algorithms mentioned above are based on conventional

feedforward neural networks. However, the conventional feedforward neural networks are trained by using gradient-based learning algorithms extensively, so their learning speed is in general far slower than required and these learning algorithms exist local minimum problems.

Extreme Learning Machine, [16], as emergent technology which overcomes some challenges faced by other techniques has recently attracted more and more attention. Consequently, the article presented an improved channel estimation based on the ELM algorithm with CO-OFDM with MIMO optical communication model. The simulation results show that the system performance of CO-OFDM is improved by using the channel estimation presented and it has relatively low complexity. A main drawback of the Coherent Optical Orthogonal Frequency Division Multiplexing (CO-OFDM) system is its sensitivity to fibre nonlinearity. Pilot Assisted Equalization model with ELM has been demonstrated capable of compensating fiber nonlinear distortion in a QPSK optical communication system. Increasingly extensive application scenarios and exponentially growing data volumes of MIMO-OFDM systems have imposed greater challenges on the speed, latency, and parallelism of channel estimation based on electronic processors. However, in optical transmission, the accuracy of channel estimation is often limited by the presence of optical noise. To increase the accuracy of channel estimation, the article proposes an ELM architecture to evaluate the channel distortion with a simulated channel response and predict the actual channel response from the receiver.

The organization of the article is as follows. In section 2, the literature survey of the study is defined. The problem definition and motivation of the work are described in division 3. In section 4, the proposed research methodology is described. In section 5, experimentation and result discussion are defined. In division 6, the conclusion of the work is described.

2 Literature Review

To know about the estimation, an Extreme Learning Machine (ELM) technique which is based on channel estimation has been introduced for the execution of the CO-OFDM channel.

[17] proposed MIMO Coherent OFDM (CO-OFDM)-based multi-beam FSO communication system operating at 40 Gbps. The modified Gamma–Gamma (MGG) turbulence modelling has been utilized for channel turbulences. The designed communication system shows considerable improvement in transmission distance by 3 km with a previously used WDM-based multi-beam FSO system. It performs better in all respects with BER 10E−11 and SNR 50 dB at a longer transmission distance of 7 km under atmospheric turbulences at 35 dB attenuation. Further, a significant reduction in geometric loss has been achieved for a given distance in varying turbulence fluctuations and the numeric values have been substantiated with Rytov variance.

[18] discussed the frequency-domain channel transmission model for PDM CO-OFDM/OQAM systems. With the analysis of the correlation of the ASE noise, we propose a combined intra-symbol frequency-domain averaging (CISFDA) channel estimation method for PDM OFDM/OQAM systems. Compared with the full-loaded frequency-domain channel estimation (FL-FD) method, the CISFDA method promotes the system robustness against the ASE noise and fibre nonlinear effect significantly. The proposed method is validated by numerical Monte Carlo simulations of the PDM CO-OFDM/OQAM system. Our new algorithm outperforms the FL-FD method in the 36 Gb/s PDM OFDM CO-OFDM/OQAM system, and the transmission distance is improved by 500 km with the bit-error-rate (BER) target at $3.8x10^{-3}$.

[19] proposed an artificial neural network least squares channel estimation algorithm (ANN_LS-CEA). Firstly, the algorithm fits the time domain waveform by ANN. Secondly, estimates the channel transfer function (TF) in the frequency domain by LS to effectively reduce IMI. Through a series of simulation test data, it can be found that this algorithm can effectively improve the overall performance of the system. Compared with the ANN-CEA, this algorithm can reduce the bit error rate (BER) performance by 50%.

[20] proposed OSSB generation can provide a tunable optical carrier-to-sideband ratio by adjusting the polarization controller and the mathematical principle is also discussed. Security of the system is improved by employing matched filter before DSP which has the property of noise rejection i.e. waveforms can be detected in presence of a jammer. Further, a comparison of the proposed system is performed with QPSK-IsOWC, DP-QPSK-IsOWC, and DP-QPSK-CO-OFDM-IsOWC systems in terms of log BER, error vector magnitude, received power, and optical signal to noise ratio. It is observed that the proposed system can cover 15,900 km at 100 Gbps at a targeted log BER of − 2.42 and provides enhanced performance. As per the author's best

knowledge, an IsOWC system with such bandwidth efficient spectrum, high performance, and security has not been reported in the past.

[21] proposed a Machine Learning (ML)-based scheme to detect and locate physical-layer eavesdropping. To improve the efficiency and accuracy of eavesdropping detection, both Optical Performance Monitoring (OPM) data and eye diagrams are adopted as input data. Three different ML classifiers are designed and tested to realize eavesdropping detection, location, and split ratio recognition, respectively. To demonstrate the feasibility of the proposed scheme, an experiment is conducted in an end-to-end fibre transmission system with Coherent Optical Orthogonal Frequency Division Multiplexing (CO-OFDM). The eavesdropping is simulated and performed by placing the optical coupler in different positions. In addition, different splitting ratios are considered, including 95/5, and 90/10. Results indicate that the ML scheme achieves 100% and 92.76% accuracy in eavesdropping detection and location, respectively.

Short-reach intensity-modulation and direct-detection (IM/DD) optical Fast-OFDM systems were examined by [22], and they developed combined channel estimation and digital linearization schemes. To transmit the 2PAM signals, the odd SCs of the training sequences were used. For 10 and 22 km length 12.5 Gbit/s SMF lines, the combined compensation technique helps to reduce BER. For the recommended IM/DD Fast-OFDM system, 3 dB at a bit error ratio (BER) of 10–3, after 22-km SMF transmission is used to increase the receiver sensitivity in comparison with the conventional IM/DD Fast-OFDM. A least mean square (LMS) algorithm has been proposed by [23], to evaluate the phase noise. The advantage of this algorithm is, the bit error rate is improved and the issue of phase ambiguity occurring by cycle slip has also been avoided.

A simple phase noise (PN) model has been proposed by [24], based on the channel effect of OFDM/OQAM and the distribution feature of intrinsic interference. An adaptive extended Kalman filter (AEKF) blind scheme has been developed based on the theory of the Kalman filter and the PN model to achieve flexibility in dynamic networks. A change in the identification of blind phase with a feedback loop has a temporal complexity that is just 1/3 that of a commercial laser with a linewidth of 200 kHz.

[25] proposed a method to estimate the blind channel approach using fast independent component analysis based on the weight function (FICA-WF) for blind interference cancellation. The existing models such as parallel factor analysis, joint parallel factor analysis, STBC-m-MIMO-OFDM, and MMSE-CMA-DFCE obtained SNR ranging from 10 to 20 dB, whereas the proposed model obtained better SNR of 9.02 dB for the FastICA-WF. [26] proposed a novel blind CE method for vehicular VLC to improve CE accuracy based on the exploitation of the channel statistics derived, by utilizing an extensive amount of data collected for different communication angles, distances, and ambient light conditions. First, the normalized channel frequency response (CFR) of the V2LC channel is demonstrated to be invariant of inter-vehicular distance, relative transmitter/receiver zenith angle, and ambient light. Then, this channel characteristic is exploited in the blind CE to improve its accuracy with a two-step estimation of the normalization factor. Extensive simulations at different vehicle speeds show that the proposed method outperforms the pilot-based and superimposed training-based CE methods in terms of spectral efficiency both for all modulation schemes and at all relative speeds. The proposed blind channel estimation (CE) method provides a 9.77% increase in the spectral efficiency, compared to the second best method, superimposed training-based CE, at 20 dB signal-to-noise ratio (SNR) and 160 km/h relative speed, for 64-Quadrature Amplitude Modulation (QAM) Direct Current-Biased Optical Orthogonal Frequency Division Multiplexing (DCO-OFDM). [27] examine the deep neural network (DNN) layers created from long-short-term memory (LSTM) for detecting the signals by learning the received signal as well as channel information. We investigate the performance of the system under various conditions. The simulation results show that the signal bit error (SER) is equivalent to and better than that of the minimum mean squared error (MMSE) and least square (LS) methods. From the aforementioned survey, the study utilized the Optical fibre transmission using coherent OFDM with FSO optical communication in the means of MIMO networks using an Extreme Learning Machine (ELM). Table 1 shows the comparative analysis of a recent work based on optical fibre communication.

Table 1. Comparison Analysis of Recent Survey Based on Optical fibre Communication

References	Objectives	Additional Techniques	Communication Source	Results
Luis Carlos Vieira *et al* 2021	2PAM-Fast-OFDM sequences are used for training a memoryless polynomial-based adaptive post-distorter	Short-reach intensity-modulation and direct-detection (IM/DD) optical Fast-OFDM systems.	Optical Fast-OFDM systems	The receiver sensitivity of the proposed IM/DD Fast-OFDM system is improved by about 3 dB at a bit error ratio (BER) of 10–3, after 22-km SMF transmission.
Xiaobo Wang *et al* 2020	The simplified phase noise (PN) model for OFDM/OQAM under channel effect is deduced according to the distribution feature of intrinsic interference.	New adaptive extended Kalman filter (AEKF) blind scheme to meet the demand for flexibility in dynamic networks	Orthogonal frequency-division multiplexing offset-quadrature amplitude modulation (OFDM/OQAM)	The laser linewidth is 200 kHz, and its time complexity is only 1/3 of that of a modified blind phase search with the feedback loop.
Xi Fang *et al* 2022	Frequency-domain channel transmission model for PDM CO-OFDM/OQAM systems	Combined intra-symbol frequency-domain averaging (CISFDA) channel estimation method	Multiplexed coherent optical OFDM	Transmission distance is improved by 500 km with the bit-error-rate (BER) target at $3.8x10^{-3}$.
Xiaoyu Wang *et al* 2022	Artificial neural network least squares channel estimation algorithm (ANN_LS-CEA)	The channel transfer function (TF) in the frequency domain by LS	Multiplexing/offset quadrature amplitude modulation (OFDM/OQAM) passive optical network (PON)	Reduce the bit error rate (BER) performance by 50%.
Simarpreet Kaur *et al* 2022	Proposed OSSB generation to provide a tunable optical carrier-to-sideband ratio	QPSK-IsOWC, DP-QPSK-IsOWC, and DP-QPSK-CO-OFDM-IsOWC systems	Optical single sideband (OSSB) modulation-based dual polarized (DP) Mach–Zehnder Modulators and polarizer	15,900 km at 100 Gbps at a targeted log BER of -2.42

3 Research Problem Definition and Motivation

The key technique is channel estimation is considered in which the performance gets affected greatly in coherent optical Fiber-optic communication systems. The original signals can be recovered, by transmitting the known information from the transmitter to the receiver and by adjusting

some effects like dispersion, nonlinearity, loss, etc. The orthogonality is destructed present in between the subcarriers and hence the signals found in the sub-channels may interfere with each other in the OFDM system. The OFDM system's vulnerability to frequency deviation is one of its fundamental flaws. Some advantages of the optical IMDD-OQAM-OFDM system over the intensity modulation and direct detection (IMDD) method include high spectrum efficiency due to a higher side lobe suppression ratio provided by a specially designed filter bank, the viability of asynchronous transmission and cost-effectiveness due to the use of simple transceivers. Also, OQAM-OFDM has the same symbol timing faults and carrier frequency offset compared to another type of multicarrier modulation scheme. In addition, since the OQAM-OFDM signal is transmitted in a complex channel and has real field orthogonality built in, the phase noise is made trickier and more challenging to reduce by intrinsic imaginary interference (IMI).

The prediction of the channel has been considered an essential module, to enhance the orthogonal frequency division multiplexing (OFDM) system execution. The high spectral efficiency can be acquired because there is no need for the time-frequency domain well-localized pulse shapes and CP. The frequency offset and robustness of the system are high due to the small leakage of out-of-band power in OFDM/OQAM. The benchmark pilot-assisted equaliser the fully-real ELM outperforms the RC-ELM and nearly matches the ELM well-defined in the common phase error (CPE) and the complex domain (C-ELM) compensation in terms of the BER over an additive white Gaussian noise channel and several laser oscillators. Some disadvantages were categorized based upon both techniques namely: An extra prelude is essential for channel estimation purposes whereas the transmission rate is reduced by the compensator, and the C-ELM needs finite and activation function which would be identifiable. The CPE compensator and C-ELM are more competitive than the unique ELM algorithm in this case for the quadrature amplitude modulation with 16-ary.

4 Proposed Research Methodology

Multicarrier techniques have attracted much interest in high-speed optical communication systems, due to their higher spectral efficiency and enhanced tolerance to dispersion. Coherent optical orthogonal frequency-division multiplexing (CO-OFDM) has been recently proposed to combat fibre chromatic dispersion and polarization-mode dispersion (PMD). CO-OFDM offers the advantages of high electrical and optical spectral efficiency, dispersion insensitivity, high optical signal-to-noise ratio (OSNR) sensitivity, and computation efficiency. Channel estimation and equalizations are the most important process on the receiver side of all kinds of communication networks to estimate the characteristics of the channel. In this work, a new technique is proposed to perform the channel estimation technique to improve the BER performance for high-speed data communication networks based on coherent optical orthogonal frequency division multiplexing (CO-OFDM). The proposed work investigates an Extreme Learning Machine-based channel estimation model, which varies in terms of performance, complexity, and tolerance to system impairments, to find out the optimal design. Figure 1 illustrates the block diagram of the proposed work.

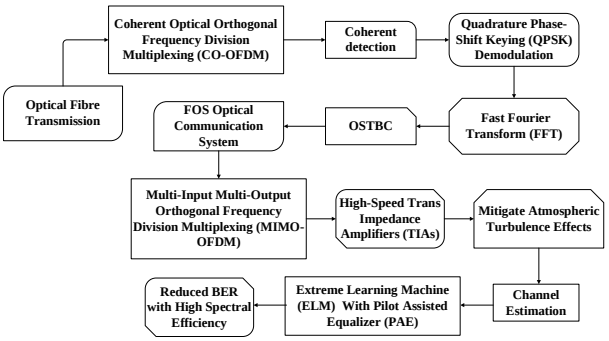

Fig. 1: Block Diagram of the Proposed Work

A coherent optical (CO) orthogonal frequency division multiplexing (OFDM) scheme gives a scalable and flexible solution for increasing the transmission rate, being extremely robust to chromatic dispersion as well as polarization mode dispersion. Further, the research utilized coherent multiple-input multiple-output (MIMO) architecture for optical wireless communications (OWCs) to mitigate atmospheric turbulence effects. The beam intensity profile was measured for investigating the temporal nature of atmospheric turbulence on the optical beam. Transmitter optical signals operate at distinct carrier frequencies to allow the received optical signals to be separately processed. It increases the channel capacity of the system almost linearly with the number of transmitting antennae. High-speed Trans Impedance Amplifiers (TIAs) used at the front end of optical fibre receivers present design challenges in the form of trade-offs between input noise current, speed, trans-impedance gains, power dissipation, and supply voltage. Coherent detection is usually considered necessary

to alleviate this trade-off. Accordingly, the study utilized quadrature phase-shift keying (QPSK) with coherent detection, this has the same sensitivity as binary phase-shift keying (BPSK) but doubles the spectral efficiency. However, it has been shown that OFDM is sensitive to phase noise. Specifically, the phase noise will cause common phase error (CPE) noise and inter-carrier interference (ICI). The CPE can be estimated by the pilot-assisted (PA) approach. At the CO-OFDM receiver after removing CP and implementing the FFT operation, it is followed by a channel estimation operation. The study utilized Extreme Learning Machine (ELM) for channel estimation, which improves the BER performance and reduces the signal peak-to-average ratios when the fibre nonlinearity becomes significant. The simulation results illustrate that the proposed CO-OFDM-ELM system has better BER performance with high spectral efficiency and less computational complexity.

4.1 Coherent Optical OFDM Network

The optical domain OFDM coherent identification and modulation are used to accomplish CO-OFDM. It has good receiver sensitivity and spectral efficiency performance. A coherent optical OFDM system's block diagrams are shown in Figure 2. The random sequence generator will generate the random sequence in the proposed system. To produce padding bytes and blinding values, a vital role is performed in cryptography algorithms like private key pairs or authentication protocols.

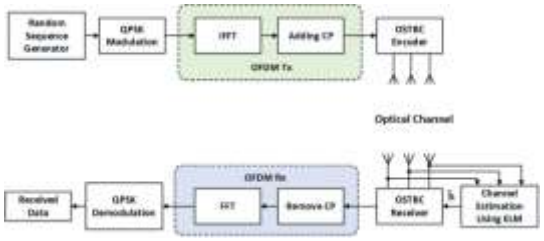

Fig. 2: Block Diagram of Coherent Optical OFDM System

Further, QPSK modulation is performed on the sequence that is generated by the random sequence generator. By swapping the stage of a constant frequency reference signal, the data can be carried out in a digital modulation process. The modified signal is employed by the IFFT as the signal from its original domain is transferred by Fourier analysis transforms, which is frequently time or space, to a portrayal in the frequency domain and vice versa. In the next step add pilot data to the original data. Every polarization consists of training symbols which are data and each training symbol contains a special pilot structure to evaluate the channel distortion and IQ mismatch factors. Data along with the pilot is sent to the OSTBC encoder and the encoded data is sent to the optical channel.

At the receiving end from the channel, the distortion $d^{'}$ is identified by the special block channel estimation using ELM and the value of distortion $d^{'}$ is sent to the OSTBC receiving end based on the distortion information the data is decoded and pilot data is removed. FFT is implemented in the data and QPSK demodulation is done in the data to get its original form.

In the P_E data pipes, the serial data input is transmitted at the transmitter end and it is depicted to corresponding constellation symbols. Following the data streams, the P_q pilot subcarriers, pilot subcarriers were inserted gradually. To establish the digital time-domain signal, the inverse FFT is used, which is then merged with a cyclic prefix (CP) to reduce the interruption of the inter-symbol caused by multipath channels. By employing an ideal digital-to-analogue converter (DAC) with a correct sampling rate, such as an OFDM transmitter the real-time waveform is then produced. For the OFDM symbol, the baseband signal is described in equation (1).

$$a_1(u)=\sum_{l=0}^{P_t-1} e(m)\exp\left(j2\pi g_m u\right) \quad (1)$$

Where, $e(m)$ and g_m denotes the data that is transmitted and the frequency of subcarrier at the m subcarrier and number of subcarriers are shown by $P_t=P_E+P_q$. The subcarrier index $e(m)$ needs to be modulated $e_E(m)$ or unmodulated $e_q(m)$. As indicated, reference tones $e_q(m)$ are gradually attached along with the data subcarriers $e_E(m)$ through the OFDM symbols for clarification purposes. $1/U=g_m-g_{m-1}$ shows the differences between the nearby subcarriers which will be orthogonal, in which the time taken by the one OFDM symbol is denoted U.

Because of the presence of a laser oscillator, there was a difference noted in the phase noise in which the optical-up conversion stage has been optimised. By a single-frequency laser, the modulated signal $F_N(u)$ is stated in equation (2).

$$a_2(u)=F_N(u)a_1(u) \quad (2)$$

Therefore, $a_2(u)$ can be rewritten as

$$a_2(u)=R_N \exp\left(j\left[2\pi g_N u+\theta_1(u)\right]\right)\sum_{l=0}^{P_t-1} e(m)\exp\left(j2\pi g_m u\right) \quad (3)$$

Equation (3), R_N denotes the optical tone amplitude, g_N denotes the optical carrier frequency, and $\theta_1(u)=\int_{-\infty}^{u}\varphi x_1(\rho)\,d\rho$ the noise present in the laser phase. $\varphi x_1(u)$ is the noise of frequency with the values of autocorrelation and zero mean function equals to $2\pi\Delta y_1\,\varphi(\rho)$, were Δy_1 , and $\varphi(\rho)$ are considered as the Dirac delta method and laser linewidth framework. At the coherent receiver, an optical OFDM signal and a local oscillator are integrated through fibre optics. $a_3(u)$ can be rewritten in equation (4) as

$$a_3(u)=s(u)*a_2(u) \quad (4)$$

With $*$ and $s(u)$ refers to the impulse reaction of the convolution process and optical channel. Each fibre span confined a chromatic dispersion, several stages of high birefringence devices, and polarization dependent on loss components. The final result of fibre chromatic dispersion leads to the generation of phase error which must be considered that concludes a time-invariant phase rotation which can be removed by a critical multiplication in the OFDM receiver and hence the channel response is assumed as, $a_3(u)=\varphi(u)*a_2(u)=R_N \exp\left(j\left[2\pi g_N u+\theta_1(u)\right]\right)\sum_{l=0}^{P_t-1} e(m)\exp\left(j2\pi g_m u\right)$. In the optical domain, if the OFDM signal bandwidth is less than the RF it might be taken as a strict sense which is most common in the OFDM signals. The laser phase noises mainly damage the execution of the CO-OFDM and hence to improve the ELM our study mainly focuses on it. Since the effects of fibre nonlinearities and chromatic dispersion on BER depend upon the subcarrier position, the results of optical channel models with linearities and nonlinearities exist must be noted. The coherent detection should be noted which defines heterodyning the optical signal in which the photodetector holds the continuous-wave optical field $F_{NV}(u)$ and hence the electrical current is given in equation (5).

$$a_4(u)=T\left|F_{NV}(u)+a_3(u)^2+v(u)\right| \quad (5)$$

The above equation can be derived as

$$a_4(u)=T\begin{pmatrix} R_{NV}^2+R_N^2\left|\sum_{l=0}^{P_t-1} e(m)\exp\left(j2\pi g_m u\right)\right|^2+ \\ 2R_{NV}R_N\,\Re\left\{\sum_{l=0}^{P_t-1} e(m)\exp\left(2\pi(g_{wG}+g_m)u+\theta_{WG}(u)\right)\right\}\end{pmatrix}+i(u) \quad (6)$$

Where, the responsivity of the photodiode is represented by R, where R_{NV}, g_{NV} and $\theta_2(u)$ denotes the local oscillator's amplitude, frequency, and phase. $\Re$ is the function of the real part, $g_{wG}=g_N-g_{NV}$ implies the RF and the phase noise of RF is $\theta_{WG}(u)=\theta_1(u)-\theta_2(u)$, with linewidth Δz_{WG} which again is seen through the subcarriers with Lorentzian spectra and is produced by the laser linewidth and local oscillator linewidth. Additionally, $i(u)$ refers to the AWGN signal which is still found in the receiver and used to detect the thermal and shot noises. If the low frequencies have been hidden, the Hilbert transform has been used to convert the signal to an analytical representation, and the baseband frequency has been applied, for the OFDM demodulator the is given in equation (7).

$$a_5(u)=\exp\left[j\theta_{GW}(u)\right]\sum_{l=0}^{P_t-1} e(m)\exp\left(j2\pi g_m u\right)+i^*(u) \quad (7)$$

Where, $i^*(u)$ represents the baseband AWGN signal, and through the SNR the frequency domain is determined.

To pretend the ADC process, the symbol of OFDM is sampled using a fixed sampling rate and by using the demodulation process, time and frequency synchronization are assumed, hence the CP is rejected and FFT is executed. The m th arrived information symbol can be stated in equation (8).

$$\overline{e(m)}=\vartheta(0)e(m)+K(m)+P^*(m) \quad (8)$$

Where, $\vartheta(0)$ represents the RF phase noise dc portion, called CPE term, $K(m)=\sum_{n=0,n\neq m}^{P_t-1} e(n)\vartheta(m-n)$ denotes the coefficient of ICI coupling in between two subcarriers with a distance m, and $I^*(m)$ represents AWGN on the m th subcarrier. $\vartheta(n)$ is described in equation (9) as

$$\vartheta(n)=\frac{1}{P_t}\sum_{i=0}^{P_t-1}\exp\left\{j\left[\theta_{GW}(i)-2\pi in/P_t\right]\right\} \quad (9)$$

With $\theta_{GW}(i)$ being the RF phase variation is obtained from discrete time. All the subcarriers of

the OFDM symbol must be taken into account and hence equation (9) was represented in a compact matrix form as:

$$\overline{R\,P_{t\times 1}} = Z_{P_t \times P_t}\, R_{P_t \times 1} + P^{*}_{P_t \times 1} \quad (10)$$

In the OFDM spectrum, for the estimation of time-varying channels, a particular number of subcarriers are allocated. In the PAE methodology, the values were given by the pilots which are used in the linear interpolation for the detection of the output of channel frequency for the data subcarriers as described in the introduction. High performance and low complexity can be defined through this equalization method. The average power of the constellation derives from the strength of pilot subcarriers and for the sake of simplicity, the pilot's quadrature component is set to 0. In the PAE technique, in a single constellation point, all the other reference tones are present. The phase noise for OFDM symbols can be decreased by the equalizer especially when ICI dominates the CPE.

4.2 MIMO-Based Optical Communication

The MIMO-based optical communication system is demonstrated as the transmitter consists of b antennas, the receiver contains c antennas, where all the symbols that were transmitted share m subcarriers. Figure 3 shows the MIMO-based communication in optical channels. The sequence of frequency-domain transmitted from the $l\,th$ $(l=1,\ldots,l)$ transmit antenna is represented by B_l, m, where $(m=1,\ldots,m)$ represents the $m\,th$ subcarrier of OFDM. The received signal of OFDM is stated in equation (11) as

$$D_{b,c} = \sum_{l=1}^{L} H_{b,l,m}\, D_{l,m} + \phi_{b,c} \quad (11)$$

Where the response of frequency in the channel between $b\,th$ transmit antenna and the $c\,th$ receive antenna for the $l\,th$ subcarrier is $H_{b,l,m}$, the frequency response of zero-mean additive white Gaussian noise (AWGN) with a one-side power spectral density is denoted by $\phi_{b,c}$. $B_l = \left[B(1,m), B(2,m), \ldots, B(l,m)\right]^T$ denotes the signal transmitted on the $l\,th$ subcarrier from all the L transmit antennas, where T represents transpose. The CSI matrix D_c of the received can be defined in equation (12) as

$$D = \left[D_1^Y, D_2^T, D_3^T, \ldots, D_N^T\right]^T = H_b\, b_l + \phi \quad (12)$$

Where H represents the block diagonal axis.

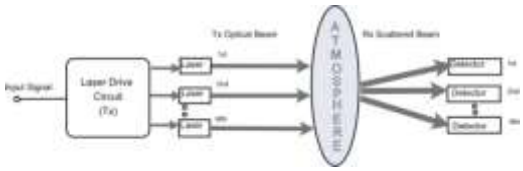

Fig. 3: MIMO-Based Optical Communication

To clarify the whole photodetector array, an assumption is made as on the receiver side the beam spots are viewed as wide. The issue of transmitter-receiver pointing has been resolved by this approach. Furthermore, in a Trans impedance amplifier (TA), a positive-intrinsic-negative (p.i.n.) photodetector is set up for the receiver's implementation. By the recurrence of MIMO, the photodetector output scheme p can be represented in equation (13).

$$y_n(l) = x(l)\sum_{m=1}^{M} I'_{nm} + z_n(l), \quad x(l) \in \{0, \mathrm{K}\} \quad (13)$$

The pulse intensity during the absence of scintillation is represented by K and at the th period, the data symbol is denoted by $x(l)$. In between the m th $(m=1,2,\ldots,M)$ optical source and the th photodetector $(n=1,2,\ldots,N)$ I'_{nm} denotes the intensity channel coefficient. The gamma-gamma probability density function is described in equation (14).

$$f(I') = \frac{2(\alpha\beta)^{(\alpha+\beta)/2}}{\Gamma(\alpha)\Gamma(\beta)}\, I'^{(\alpha+\beta)/2-1}\, \mathrm{E}_{\alpha-\beta}\left(2\sqrt{\alpha\beta I'}\right) \quad (14)$$

Where the signal intensity is denoted by I', the gamma function is denoted by $\Gamma(.)$ and the second kind of modified Bessel function is denoted as $\mathrm{E}_{\alpha-\beta}(.)$. For the order $\alpha-\beta$, the parameters of the scintillation experienced by plane waves and for zero inner scales can be denoted by α and β.

The transmitted symbols of different types may meet various atmospheric turbulence conditions and based upon that the optical sources were located. For the TA thermal noise, the n th receiver is represented as z_n in which the double-side power spectral density $N_0/2$ was modelled by zero-mean Gaussian process.

Atmospheric Turbulence Channel

The atmospheric turbulence for the vertical FSO link becomes weaker as the altitude of transmissions increases, consequently, the model assumed the log-normally distributed channels for the weak turbulence regime is stated in equation (15) as

$$I^{mn} = e^{Z_{mn}} \quad (15)$$

Where, Z_{mn} is a Gaussian random variable with the mean $\mu_{Z_{mn}} = \mu_Z$ and the variance $\sigma^2_{Z_{mn}}$. Assume that $\mu_{Z_{mn}} = \mu_Z$ and $\sigma^2_{Z_{mn}} = \sigma^2_Z$ for all $m \in \{1, \cdots, M\}$ and $n \in \{1, \cdots, N\}$ for the independent and identically distributed channels. The Rytov variance $\sigma^2_Z = -\mu_z/2$ for each transceiver to ensure $E\{I^m\} = 1$ is (equation 16)

$$\sigma_Z^2 = 2.25k^{\frac{7}{6}}(L - h_0)^{\frac{5}{6}} \times \int_{h_0}^{L} C_n^2(l)\left(\frac{l-h_0}{L-h_0}\right)^{\frac{5}{6}}\left(\frac{l-h_0}{L-h_0}\right)^{\frac{5}{6}} dl \quad (16)$$

Where, $k = \frac{2\pi}{\lambda}$, $\lambda, L,$ and h_0 are the wavelength, the altitude of the photodetector, and the ground. The perpendicular environment is assumed to make the transmission distance equal to the altitude of the photodetector for the vertical link. Note that the atmospheric channels for all diversity channels are independent of the distance between the transmitters or receivers and larger than the coherence length. Therefore, the detected misalignments for the N receivers are also independent. The sum of the log-normal random variable of received powers could be approximated to a single log-normal random variable using Wilkinson's method. Further, the averaged centroid can be approximated in equation (17)

$$\Delta x_{ac} = \frac{1}{N}\sum_{n=1}^{N} \Delta x_{ac,n} = \frac{1}{N}\sum_{n=1}^{N} S \quad (17)$$

Where S is the Gaussian distributed statistical misalignment model with a zero mean and the variance $\sigma^2_{c,n}$of aggregated centroid $\Delta x_{ac,n}$. The detected centroids for each receiver are independent, the mean of the averaged centroid is zero, and the variance of the overall detected misalignment error can be expressed in equation (18) as

$$\sigma_c^2 = \sum_{n=1}^{N} \frac{\sigma^2_{c,n}}{N^2} \approx \frac{\left(e^{\sigma_Z^2} - 1\right)d^2}{8\left(e^{\sigma_Z^2} - 1 + M\right)Nsin^2(\pi/M)} \quad (18)$$

The pointed direction of the transmitted beam is assumed to aim at the centre of the receiver distributions. The channel gain for M×N MIMO-based FSO transmissions can be expressed in equation (19) as

$$H = \sum_{m=1}^{M}\sum_{n=1}^{N} H_{mn} = \sum_{m=1}^{M}\sum_{n=1}^{N} A_0 e^{Z_{mn} - 2R^2_{mn/w^2}} \quad (19)$$

Where ω and H_{mn} are the beam width and the radial displacement of the m[th] transmitted beam at the n-th receiver due to a pointing error. The outage of the transmitted signal is defined as the received power becoming less than the receiver sensitivity.

4.3 Channel Model of CO-OFDM

The Spatial sub-channels were presumed, independent. The assumed condition is reasonable if the spacing of the antenna is larger than half of the carrier wavelength.

An exponential power-delay profile has been designed in IEEE 802.11. The difficult 3D environments can be designed by the Optic studio which is the advantage of this method. The output of the ray-tracing method contains the database file in brief of the created rays, in which the strength and length of the optical path preceding each reflection are also contained in it. In CIR, $h(t)$, can then be determined in equation (20)

$$h(t) = \frac{1}{N_{rays}} \sum_{i=1}^{N_{rays}} P_r, l^o \left(t - \frac{d_i}{c}\right) \quad (20)$$

Here, c denotes the speed of light and the total distance is denoted by d_i whereas before getting into the detector the i th ray has been traveled, $h(t)$ denotes the Multi Carrier Modulation (MCM) transmitted signal, t defines the symbol period. To analyse the retrieved simulation results, several metrics were used in which the DC of channel profit and delay spread is also given. The DC expansion H_0 is stated in equation (21) as

$$H_0 = \int h(t)dt \quad (21)$$

H_0 denotes the frequency of the subcarrier, Also, the spread τ_0 of the channel is delayed by the root means squared (RMS) delays τ_0 is represented in equation (22).

$$\tau_0 = \sqrt{\frac{\int_0^{\infty}\left(t-\tau\right)^2 h^2(t)dt}{\int_0^{\infty} h^2(t)dt}} \quad (22)$$

Where, r denotes the mean excess delay, described by (23).

$$r=\frac{\int_0^\infty t\,h^2(t)dt}{\int_0^\infty h^2(t)dt} \tag{23}$$

To fit the histogram of the network gains to a certain probability density function (PDF), such as lognormal, Nakagami, Rayleigh, Weibull, etc., statistical modelling for the dynamic WBAN channels must take this into account. AIC denotes the Akaike Information Criterion which is expressed in equation (24) as

$$AIC=-\log\times L(\Theta|x)+2p+\frac{2p(p+1)}{N_p-p-1} \tag{24}$$

Where, the log-likelihood of the predicted model with the parameter Θ of size p is represented by $\log\times(L(\Theta|x))$, the limitation on the models of data x of size N_p. The method that fits the data corresponds to the smallest AIC score. The time interval for which the autocorrelation function (ACF) is below a particular threshold is defined as channel coherence time, to define channel time fluctuations.

4.4 Channel Estimation Using ELM

ELM-based channel estimation is a very efficient calculation for the distortion in optical channels, better accuracy is obtained while using this kind of method. The input parameters are given to the ELM machine by using this parameter for training and testing. There is a correlation between different parameter levels so all the factors of the direct communication network have to be configured, which makes direct transmission neural network prediction accurate. The ELM is a learning algorithm for feed-forward artificial neural networks characterized by a single hidden layer. The ELM tends to minimize the training error with the adoption of the smallest norm of the output weights. In addition, the ELM has a fast learning speed, as the only parameters that need to be optimized are the output weights between the hidden neurons and the output layer. The computational time required for training can be considered negligible in comparison with traditional feed-forward neural networks and support vector machines. The ELM refers to an attractive learning algorithm for SLFNs, which has fast training speed together with good generalization performance. It is characterized by the random assignment of the weights of the input layer as well as the threshold values in the hidden layer and, hence, the training problem is translated into finding the minimum norm least-squares solution of a linear system. The basic ELM may be written as follows (25).

$$f(x)=\sum_{i=1}^{L}\beta_i g_i(x)=g(x)\beta=T \tag{25}$$

Where the weight of the resultant matrix is denoted by β, T represents the target output matrix, $g(.)$ which represents the activation function. Figure 4 shows the network structure of ELM.

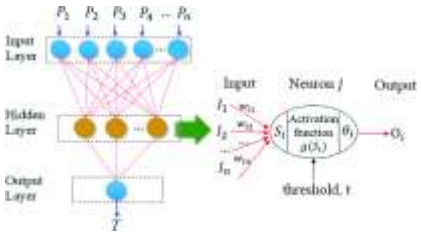

Fig. 4: ELM Network Structure Model

Since the nodes hidden in the ELM training parameters are randomized and remain unchanged during the training procedure, ELM may not reach the optimal classification limit. ELM has been able to improve sorting performance, reduce the misclassified samples, and reduce variation between different implementations.

$$f_L(x)=\sum_{i=1}^{L}\beta_i h_i(x) \tag{26}$$

Where the output weight of the i th has hidden node is represented by β_i and f_L denotes the hidden layer of the output function in (26). Here, for the ELM the secret layer has been shown, i th resultant hidden node is x_i, the parameters of the i th has hidden node is w_1 and b_1. The fundamental ELM can be written in equation (27) as

$$\begin{bmatrix} g(w_1.x_1+b_1) & \cdots & g(w_L.x_1+b_L) \\ \vdots & g(w_j.x_i+b_j) & \vdots \\ g(w_1.x_N+b_1) & & g(w_L.x_N+b_L) \end{bmatrix}\begin{bmatrix}\beta_1^T\\ \vdots\\ \beta_L^T\end{bmatrix}=\begin{bmatrix}t_1^T\\ \vdots\\ t_N^T\end{bmatrix} \tag{27}$$

Where H is the output matrix of the hidden layer, β is the output weight matrix, T is the matrix of the target output, $g(\cdot)$ refers to the activation function, $w_j=[w_{j1},w_{j2},\ldots,w_{jn}]^T$ defines the weight vector in between the j th input and the hidden nodes, $x_i=[x_1^i,x_2^i,\ldots,x_n^i]^T\in\Re^n$ denotes i th information for n-dimensional input data, the inner product between w_j and x_i is defined by a term, the bias of the j^{th} hidden neuron is b_j,

$\beta_j = [\beta_{j1}, \beta_{j2}, \ldots, \beta_{jm}]^T$ which refers to the weight of resultant vector lies in between the j^{th} has hidden node and the output neurons and $t_i = [t_1^i, t_2^i, \ldots, t_m^i]^T \in \Re^m$ represents the m-dimensional target vector ensured from x_i. The ELM training approach creates a model for single hidden layer sigmoid neural networks Y as a particular case is defined in equation (28).

$$Y = W_{2\sigma}(W_{1x}) \tag{28}$$

Where, W_1 the matrix of input-to-hidden-layer weights is represented by, σ denotes the activation function, and the matrix of hidden-to-output-layer weights is represented by W_2.

In the ELM algorithm, input weights w_i and bias b_i are randomly generated according to a probability distribution and are related by the inner product operator. Generally, for a given training set with Nm instances$\{U, T\} = \{u_i, t_i\}_{i=1}^{N_m}$, where $u_i = [u_{i1}, u_{i2}, \cdots, u_{iD_i}] \epsilon \mathbb{R}^{D_i}$ is an input sample and $t_i = [t_{i1}, t_{i2}, \cdots, t_{iD_0}] \epsilon \mathbb{R}^{D_0}$is its corresponding output (the input dimension D_i and output dimension D_0 are not necessarily equal),

The training process of the ANN can be expressed as a linear regression problem for the ELM algorithm, where a zero training error between the target output and the actual output $\left(\sum_{i=1}^{N_m} t_k - \hat{t}_k\right)$ can be determined as follows (29).

$$T = F\beta_{ELM} \tag{29}$$

The optimal solution to the ELM can be computed in equation (30).

$$\beta_{ELM}^* = F^{\dagger}T \tag{30}$$

Where $F^{\dagger}$is the Moore-Penrose generalized inverse of F. If we consider zero training error, over-fitting could appear in the ELM algorithm. To avoid this problem, calculations are done by minimizing the final weights β_{ELM} with the inclusion or a regularization parameter. In other words, the mean square error is given by equations (31, 32).

$$\min_{\beta_{ELM}, e} \frac{1}{2}\|\beta_{ELM}\|^2 + \frac{C}{2}\sum_{i=1}^{N_m}\|e_i\|^2 \tag{31}$$

$$\text{s.t } f(u_i)\beta_{ELM} = t_i^T - e_i^T, i = 1, \cdots, N_m \tag{32}$$

Where, $f(u)$ represents an $output(row)$ vector of the matrix in expression, $e_i \in \mathbb{R}^{d_0}$is the error vector concerning the ith input sample, and C corresponds to the penalty coefficient, which must be any real positive number. Here, F denotes the actual output and T defines the target output. Finally, its solution when F has more rows than columns ($n_h > N_m$), can be written as follows (33).

$$\beta_{ELM}^* = \left(F^T F + \frac{I_{n_h}}{C}\right)^{-1} F^T T \tag{33}$$

Where, I_{n_h} is an identity matrix with dimension n_h. n_h denotes the number of hidden neurons. On the other hand, in the case, that F has fewer rows than columns ($n_h > N_m$), the previous solution can be written in equation (34) as

$$\beta_{ELM}^* = \left(FF^T + \frac{I_{N_m}}{C}\right)^{-1} T \tag{34}$$

Where, β_{ELM}^* signifies the optimal solution of ELM. Thus to improve the accuracy of the predictions model, the expressions for β_{ELM} shown above are obtained when modifying the problem on equation (31), this depicts that

$$\min_{\beta_{ELM}, e} \frac{1}{2}\|\beta_{ELM}\|^2 + \frac{1}{2}\sum_{i=1}^{N_m} C_i\|e_i\|^2 + \frac{\lambda}{2}T_r(\beta_{ELM}^T F^T L F \beta_{ELM}) \tag{35}$$

$$\text{s.t } f(u_i)\beta_{ELM} = t_i^T - e_i^T, i = 1, \cdots, N_m$$

Finally, the last step is to perform MIMO combining with the trained ELM output weight vector illustrated in equation (36).

$$\hat{s}_k = O_{s,k}\beta_k \tag{36}$$

Where, $\hat{s}_k = \{\hat{s}_k[1], \cdots, \hat{s}_k[N_s]\}^t$ denotes the detected data symbols at the output layer of the ELM network. It is worth noting that w_i and b_i in (27) are fixed after the ELM training and reused for further processing.

5 Experimentation and Result Discussion

The channel estimation in a coherent optical OFDM network is imposed in MATLAB 2021a in an i5 system with storage of 4 GB RAM is defined in Table 2. The model execution is computed in terms of BER by varying the number of the antenna on the transmitting side and the receiving side. The existing method and ANN were analysed for the analysis purpose of this method. By making use of the Extreme Learning Machine (ELM) network suggested in this work, performance is improved, but security is severely compromised. Based on the accuracy, the system's performance is evaluated.

Table 2. Simulation System Configuration

MATLAB	Version R2021a
Memory Capacity	4GB DDR3
Operation System	Windows 10 Home
Processor	Intel Core i5 @ 3.5GHz

The accuracy graph is generated to determine the performance, as shown in Figure 5 by employing both the suggested method ELM and the existing ANN (Artificial Neural Network). The same number of channels and users as in the proposed way is supplied for both implementations. The performance graphs that resulted are provided below.

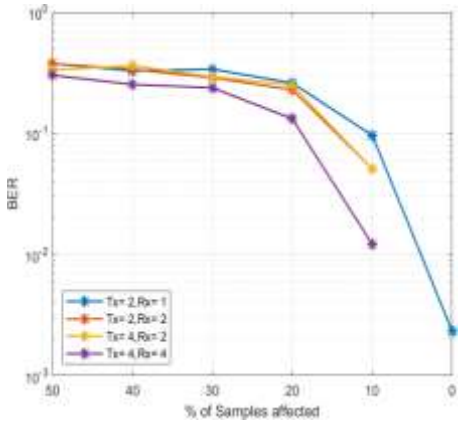

Fig. 5: BER Results Using ANN-Based Channel Estimation

According to the channel estimation method which uses the ANN method, the output of the bit error rate is deployed in Figure 5. It consists of four levels of samples, one receiver and two transmitters, two transmitters and two receivers, four transmitters and two receivers, and four transmitters and four receivers. The percentage of affected samples is approximately 10%.

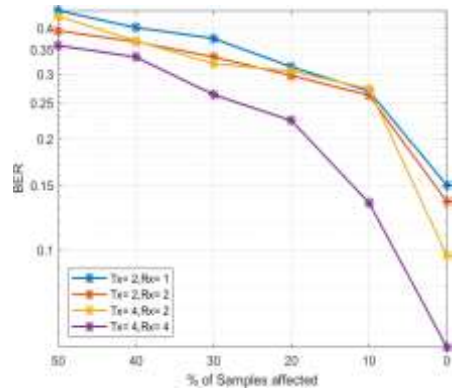

Fig. 6: Bit Error Rate without Channel Estimation

Figure 6 depicted the BER performance without channel estimation methods, i.e., there is a chance of 5% getting affected if the BER is 0.2. Then for the second and third samples, the percentage of affected samples is approximately 6. The final samples produce the percentage of affected samples are 18.

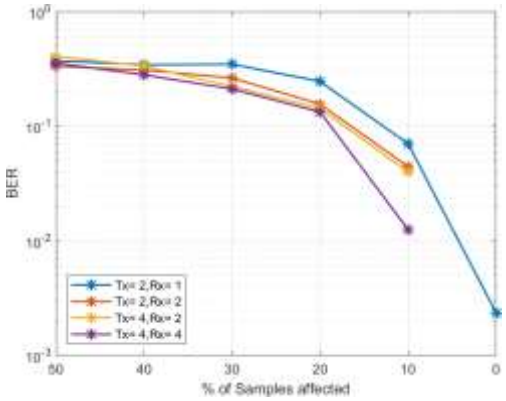

Fig. 7: BER Based On ELM Based Channel Estimation

The graph for bite error rate using an Extreme Learning Machine is illustrated in Figure 7, which consists of four transmitter and receiver samples. These samples produce the percentage of affected sample values like 13%, 16.8%, 17%, and 19% when the bit error rate is 10^{-1}, respectively.

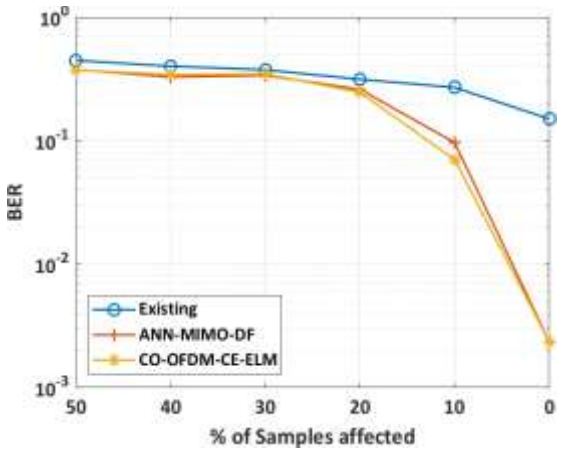

Fig. 8: BER for Two Transmitters and One Receiver

Figure 8 demonstrates the bit error rate graph using two transmitters and one receiver. Which is compared with the prevailing ANN-MIMO-DF-based methods. The proposed CO-OFDM-CE-ELM method performs better than the other methods like the existing and the ANN-MIMO-DF, respectively.

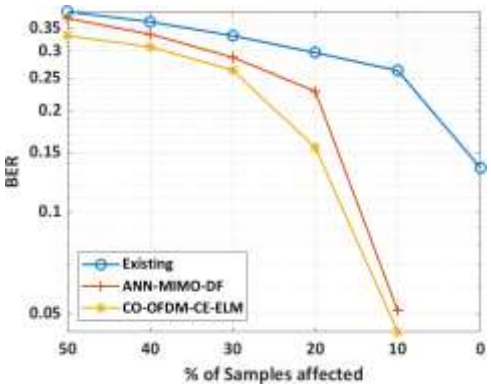

Fig. 9: BER for Two Transmitters and Two Receivers

Figure 9 depicted the bit error rate graph when it has two transmitters and two receivers. The existing method and the ANN method were compared with the developed method. When the BER is 0.2, the existing method has 0.6%, the ANN has 19.6% and the proposed method has a 25% of affected samples. While comparing to it, the proposed method has a better performance.

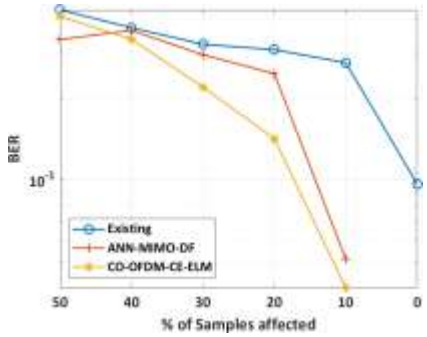

Fig. 10: BER for Four Transmitters and Two Receivers

Figure 10 shows the bit error rate values for the four transmitters and two receivers. It is compared with the already available ANN method. When the BER is 0.1, the percentage of samples affected is 0.2% for existing, 14% for ANN, and 18% for the proposed method, respectively.

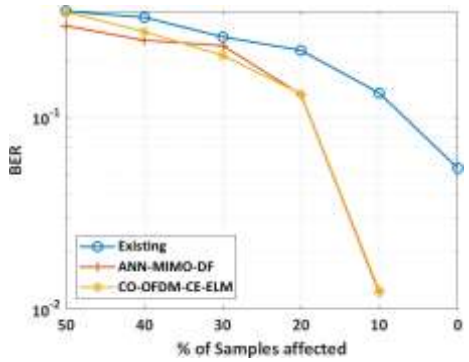

Fig. 11: BER for Four Transmitters and Four Receivers

Figure 11, reveals the bit error rate of the developed method for four transmitters and four receivers. It compares the proposed method with the existing ANN methods. For the existing method, there is a chance of 8% getting affected and for the proposed method there will be 19.5 % damage if the BER is 0.1.

6 Discussion

The channel estimation in a coherent optical OFDM network is implemented in MATLAB 2021a software. Performances of the model are measured in terms of bit error rate by varying the number of the antenna on the transmitting side and the receiving side. For analysis purposes, this method is analyzed with the existing method and ANN. [28] identified the minimum bit error rate (BER) for the 16-QAM modulation with varying fibre length. The OFDM-RoF system can be able for realizing a fibre length of 100 km with a restricted decrease in the received power so that the constellation noise becomes greater despite applying electrical amplification and optical amplification. [29] suggested the performance of OFDM with Companding is described in the Free space optical (FSO) link. The atmospheric turbulence in the FSO system is described by the Gamma-Gamma channel model. The BER performance is done with OFDM scheme with and without A-law and μ-law companding scheme in FSO medium. [30] verify the stability of the tri-directional fibre transmission system. The design of transmission methods is different wavelengths modulated in the electrical signal of 10 Gbit/s and 2.5 Gbit/s based on the corresponding architectures. BER results for different wavelengths, depicting the power penalty values at different distances from left to right, which are 0.304 dB, 0.595 dB, and 1.173 dB, respectively. It indicates that the effect of different wavelengths is much less than that of the same wavelength. [31]

illustrate that the proposed CO-OFDM-IM system has better BER performance when the proposed CO-OFDM-IM system and the CO-OFDM system have similar spectral efficiency. Also, the CO-OFDM-IM system can provide better spectral efficiency than the CO-OFDM system at low-to-medium order modulation such as BPSK, QPSK, and 16QAM. [32] results show that by reasonably setting the negotiation bit position, the consensus key could be obtained through negotiation, and the requirements of transmission performance could be met. When the negotiation bit position was set to seven, the Q-factor of the system was nine, which met the error-free condition of the 7% forward error correction (FEC) limit.

[33] present an Extreme Learning Machine (ELM)-based channel estimation (CE) approach aiming at minimizing the effective bit-error-rate (BER) for a two-user NOMA downlink system. This technique has Improved spectral efficiency (SE) and energy efficiency (EE) values can be observed for the proposed L2-norm ELM, and thus, it is proved that the ELM and L2-norm ELM-based NOMA schemes achieve a large sum capacity than other existing algorithms. [34] have the satisfactory outcome produced during the design phase is further improved by the iterative supervised learning approach. From the above discussion, it proclaims that the present article provides higher spectral efficiency with reduced BER (0.002, 0.147, 0.0316, 0.0112), (0.050, 0.0316, 0.025, 0.010) and low computational complexity with CO-OFDM-MIMO-ELM, [35].

7 Conclusion

The OFDM produced as the outcome of polarization and chromatic-mode dispersion may readily manage a high inter-symbol interference (ISI) (PMD). The OFDM can be made as a systematic technology by high spectral flexibility and spectral efficiency for the later fibre-optic links. The direct-detected and coherent optical Fast-OFDM were some other spectral-efficient modulation techniques were also presented. A new technique for channel estimation technique is proposed for CO-OFDM using ELM in this work. QPSK modulation technique is employed to perform the modulation process for the high-speed data transmission process. ELM is trained by using received data and piolet data which are used to perform the encoding process. The channel response value is predicted for each packet based on the trained elm model. Using MATLAB software, the proposed method is evaluated. To examine the proposed technique performance concerning varying probability values for SNR, the BER performance metrics are used. While the performance is compared with the already available ANN technique and found that the proposed method provides reduced BER ((0.002, 0.147, 0.0316, 0.0112) when compared to the conventional methods. Therefore, the outcome of this proposed method depicted that the execution of the proposed method is higher than the other methods, and this will useful for efficient channel estimation, respectively. The limitation of this study is that study only utilizes the BER for the analysis part. In the future, the study focuses on coherent radio signals with the OFDM visible light communication model for channel estimation. This optical fibre communication has high-speed data transmission, data security, and data reliability with various applications.

References:

[1] A. H. Ali, A. Hj, and B. S. Hassen, "Design analysis and performance evaluation of the WDM integration with CO-OFDM system for radio over fiber system," *Indonesian Journal of Electrical Engineering and Computer Science*, vol. 15, no. 2, 2019, pp. 870–878.

[2] D. Zabala-Blanco, M. Mora, C. A. Azurdia-Meza, A. Dehghan Firoozabadi, P. Palacios Játiva, and I. Soto, "Relaxation of the radio-frequency linewidth for coherent-optical orthogonal frequency-division multiplexing schemes by employing the improved extreme learning machine," *Symmetry (Basel)*, vol. 12, no. 4, 2020, p. 632.

[3] L. Wang, C. Gao, X. Deng, Y. Cui, and X. Chen, "Nonlinear channel estimation for OFDM system by wavelet transform based weighted TSVR," *IEEE Access*, vol. 8, 2020, pp. 2723–2731.

[4] J. W. Kim, J. Yoon, and S. C. Kim, "Header Information Based Channel Estimation for Highly Modulated Orthogonal Frequency-Division Multiplexing Transmissions in IEEE 802.11 ad," *Wireless Personal Communications*, vol. 115, 2020, pp. 2081–2092.

[5] L. Ge et al., "Deep neural network based channel estimation for massive MIMO-OFDM systems with imperfect channel state information," *IEEE Syst. J.*, vol. 16, no. 3, 2022, pp. 4675–4685.

[6] X. Liu et al., "Low complexity partition-recombined SLM scheme for reducing PAPR

in coherent optical OFDM systems," *Opt. Eng.*, vol. 61, no. 12, 2022.

[7] O. O. Oyerinde, "Frequency domain channel estimation schemes for PDM-coherent optical OFDM-QPSK-based communication systems," *in 2018 IEEE 87th Vehicular Technology Conference (VTC Spring)*, 2018.

[8] J. He, J. Shi, R. Deng, and L. Chen, "Experimental demonstration of OFDM/OQAM transmission with DFT-based channel estimation for visible laser light communications," *in Optics and Photonics for Information Processing XI*, 2017.

[9] Z. A. Abbasi and Z. A. Jaffery, "A weighted neuro-fuzzy hybrid algorithm for channel equalisation in the time-varying channel," *International Journal of Business Intelligence and Data Mining*, vol. 17, no. 2, 2020, pp. 237–257.

[10] X. Fang, Z. Suo, L. Zhang, Q. Zhang, and F. Zhang, "Combined phase offset channel estimation method for optical OFDM/OQAM," *Opt. Fiber Technol.*, vol. 61, no. 102390, 2021, p. 102390.

[11] S. Liang, F. Zhao, F. Zhao, Y. Huang, and C. Wang, "ANN-based channel estimation algorithm of IM/DD-OFDM/OQAM-PON systems with mobile fronthaul network in 5G," *Opt. Fiber Technol.*, vol. 59, no. 102310, 2020, p. 102310.

[12] K. Ss, "Performance Analysis of Nonlinear Fiber-Optic in CO-OFDM Systems with High Order Modulations," *IEEE Photonics Technology Letters*, vol. 30, no. 8, 2018, pp. 696–699.

[13] D. Zabala-Blanco, M. Mora, C. A. Azurdia-Meza, A. Dehghan Firoozabadi, P. J. Palacios Jativa, and S. Montejo-Sanchez, "Multilayer extreme learning machine as equalizer in OFDM-based radio-over-fiber systems," *IEEE Lat. Am. Trans.*, vol. 19, no. 10, 2021, pp. 1790–1797.

[14] J. Liu, Y. Wang, Y. Yuan, and Y. Zhang, "Channel estimation optimization algorithm based on OFDM system," *in Proceedings of the ACM Turing Celebration Conference - China*, 2019.

[15] Y. Sun and H. Ochiai, "Performance analysis and comparison of clipped and filtered OFDM systems with iterative distortion recovery techniques," *IEEE Trans. Wirel. Commun.*, vol. 20, no. 11, 2021, pp. 7389–7403.

[16] D. Zabala-Blanco, M. Mora, C. A. Azurdia-Meza, A. Dehghan Firoozabadi, P. Palacios Játiva, and I. Soto, "Relaxation of the radio-frequency linewidth for coherent-optical orthogonal frequency-division multiplexing schemes by employing the improved extreme learning machine," *Symmetry (Basel)*, vol. 12, no. 4, 2020, p. 632.

[17] Payal, D. Sharma, and S. Kumar, "Performance enhancement of multi-beam FSO communication system with the application of MIMO with CO-OFDM," *J. Opt.*, 2022.

[18] X. Fang, Y. Xia, J. Jin, M. Zhu, Z. Suo, and L. Zhang, "Combined Intra Symbol Frequency Domain Averaging Channel Estimation for Polarization Division Multiplexed Coherent Optical Ofdm/Oqam Systems," *Oqam Systems*.

[19] X. Wang, X. Wang, and H. Cao, "ANN LS-based Channel Estimation Algorithm of IM/DD-OFDM/OQAM-PON systems with SDN Mobile Fronthaul Network in 5G," *in 2022 IEEE International Conference on Communications Workshops (ICC Workshops)*, 2022.

[20] S. Kaur, "Performance analysis of DP-QPSK with CO-OFDM using OSSB generation," *Wirel. Netw.*, vol. 28, no. 4, 2022, pp. 1719–1730.

[21] H. Song et al., "Experimental study of machine-learning-based detection and location of eavesdropping in end-to-end optical fiber communications," *Opt. Fiber Technol.*, vol. 68, no. 102669, 2022, p. 102669.

[22] L. C. Vieira, S. Hussein, I. Darwazeh, C.-P. Liu, and J. Mitchell, "A combined digital linearization and channel estimation approach for IM/DD fast-OFDM systems," *Opt. Fiber Technol.*, vol. 67, no. 102725, 2021, p. 102725.

[23] M. Bharti, "Performance enhancement of coherent optical OFDM system using LMS algorithm," *J. Telecommun. Inf. Technol.*, vol. 1, no. 2020, 2020, pp. 1–5.

[24] X. Wang, L. Yang, F. Luo, S. Yang, and Y. Du, "Adaptive EKF based estimation method for phase noise in CO-OFDM/OQAM system," *IEEE Access*, vol. 8, 2020, pp. 204931–204940.

[25] R. Sindhuja and A. R. Shankar, "Massive MIMO Channel Estimation Using FastICA Weighted Function for VLC in 5G Networks," *in Series B, India*, 2023, pp. 1–8.

[26] G. Gurbilek, M. Koca, and S. Coleri, "Blind channel estimation for DCO-OFDM based vehicular visible light communication," *Phys. Commun.*, vol. 56, no. 101942, 2023, p. 101942.

[27] K. J. Wong, F. Juwono, and R. Reine, "Deep Learning for Channel Estimation and Signal

Detection in OFDM-Based Communication Systems," *ELKHA*, vol. 14, no. 1, pp. 52–59.
[28] M. M. Kareem, S. A. S. Lafta, H. F. Hashim, R. K. Al-Azzawi, and A. H. Ali, "Analyzing the BER and optical fiber length performances in OFDM RoF links," *Indones. J. Electr. Eng. Comput. Sci*., vol. 23, no. 3, 2021, p. 1501.
[29] A. H. Malini and M. Selvi, "BER Performance Analysis of OFDM Based Free Space Optical Communication System using μ-Law and A-Law Methods," *in 2022 13th International Conference on Computing Communication and Networking Technologies (ICCCNT), IEEE*, 2022, pp. 1–4.
[30] H.-C. Lee, Y. Liu, S.-K. Liaw, Y.-L. Yu, and C.-H. Yeh, "Design and analyses of BER performance in a tri-directional optical transmission system," *Opt. Commun*., vol. 532, no. 129255, 2023, p. 129255.
[31] A. Güner, "Coherent optical OFDM with index modulation for long-haul transmission in optical communication systems," *IEEE Access*, vol.10, 2022, pp.46504-46512.
[32] X. Yang et al., "Combined Optical Fiber Transmission System Based on QNSC and BER-LM," *In Photonics*, vol. 10, no. 2, 2023.
[33] M. Sarkar, S. Sahoo, and S. Nanda, "Channel estimation of non-orthogonal multiple access systems based on L 2-norm extreme learning machine," *Signal, Image and Video Processing*, vol. 16, 2022, pp. 921–929.
[34] G. Borraccini, A. D'Amico, S. Straullu, F. Usmani, A. Ahmad, and V. Curri, "Iterative supervised learning approach using transceiver bit-error-rate measurements for optical line system optimization," *J. Opt. Commun. Netw*., vol. 15, no. 2, 2023, p. 111.
[35] L. Liu, L. Cai, L. Ma, and G. Qiao, "Channel state information prediction for adaptive underwater acoustic downlink OFDMA system: Deep neural networks based approach," *IEEE Trans. Veh. Technol*., vol. 70, no. 9, 2021, pp. 9063–9076.

Contribution of Individual Authors to the Creation of a Scientific Article (Ghostwriting Policy)

The authors equally contributed in the present research, at all stages from the formulation of the problem to the final findings and solution.

Sources of Funding for Research Presented in a Scientific Article or Scientific Article Itself

No funding was received for conducting this study.

Conflict of Interest

The authors have no conflicts of interest to declare that are relevant to the content of this article.